# Spectroscopic Diagnosis of Plasmas Produced by Laser Irradiation of CdO and CdO:Cu Targets

**Hiba M. Salman**
**Falah H. Ali**
**Kadhim A. Aadim**

*Department of Physics, College of Science, University of Baghdad, Baghdad, IRAQ*


***This work aims to evaluate the effect of Nd:YAG laser beam energy on the properties of plasma that is formed by directing the laser beam on a solid target (pure cadmium oxide and copper-doped cadmium oxide) in air under influence of atmospheric pressure. Plasma is formed throughout the use of laser pulses with different energies (500, 600, and 700mJ). The emitted light is collected using a fiber cable and illuminates the entry hole of the scaled spectrometer equipped with a charged-coupled device (CCD) camera coupled with an intense charge of photoionization at multiple delay times. Electron density, electron temperature, and Debye wavelength are calculated according to Boltzmann equations.***

**Keywords:** Cadmium oxide; LIPS; Boltzmann equation; Plasma parameters
**Received:** 05 October 2023; **Revised:** 05 November 2023; **Accepted:** 12 November 2023

## 1. Introduction

Laser-induced plasma spectroscopy (LIPS) can be regarded as tried-and-true analytical technique to fast determine samples' elemental composition. LIPS can alternatively be described is an atomic emission spectroscopy form that can be utilized in order to study any material type [1]. In LIPS, the target material is excited and ionized by plasma that is formed by laser beam fixed on its surface. At once following the photons from laser beams striking the surface of target, plasma is emitted from surface material [2]. Some of the atomic and molecular types can be optically detected by investigating emission spectra from the laser-induced plasma [3].

The analytical effectiveness of LIPS is significantly influenced by a number of particular variables and characteristics, including (laser wavelength, laser power, target type, ambient gas pressure), among others [4]. Using the use of optical fibers, one may watch and analyze the characteristic light that atomic components originate [5]. A lot of notices have recently been paid to optical emission spectroscopy, which is used in LIPS-dependent relative depictions [6]. Plasma is formed as energy from laser pulse warms, atomizes, ablates, and ionizes sample material. A detector and a spectrograph are utilized afterwards in order to spectrally study and analyze plasma plume. Qualitative and quantitative information, like ingredient composition, may be assumed from resulting plasma spectra. The plasma temperature and electron density can be ascertained from the emission line's characteristics, like its shapes, width, and variations [7]. The ratio approach is one of the most often used optical emission spectroscopy (OES), and

The Boltzmann's equation is used to find the electron temperature as [8]

$$Ln\left[\frac{\lambda_{ji}I_{ji}}{hcA_{ji}g_j}\right] = \frac{1}{k_BT}(E_j) + Ln\left[\frac{N}{U(T)}\right] \quad (1)$$

where $g_j$ is high-level statistical weight from the transitional stage, and $I_{ji}$ represents relative emission line density between $i$ and $j$ energy levels. The wavelength is $\lambda_{ji}$ (in nm), $E_j$ is the excitation energy for level $j$ (in eV), $A_{ji}$ represents the potential for the automatic radiation transmission from $i$ to $j$ level, $N$ represent the population density, and $k_B$ is the Boltzmann's constant

Stark effects are formed in laser-induced plasma by electrical field, mainly due to the collisions of electrons, with small contributions that come from ion collisions. This equation can be represented as more simply as [9]:

$$n_e = \left(\frac{\Delta\lambda_{FWHM}}{2w}\right)N_r \quad (2)$$

Theoretically, the full width of Stark parameter is represented by the line $w$, $N_r \approx 10^{17}$ cm$^{-3}$, where FWHM represents the full-width at half maximum of the spectral line. Plasma frequency is set up so that any disruption of its semi-neutral equilibrium would consequence in generation of electric fields. This frequency is a very fundamental plasma factor, since it only depends on the density of the plasma. The equation below [10] can be used to compute plasma frequency that is naturally very high due to small size of m

$$f_p = \sqrt{\frac{e^2 n_e}{\varepsilon_0 m_e}} \quad (3)$$

where $\varepsilon_0$ represents free space permittivity, $n_e$ represents the electron density, and $m_e$ represents the electron mass. The essential property of plasma behavior is recognized as the Debye length ($\lambda_D$), which measures the area of an individual body

  

affecting a different body carrying an opposite charge in the plasma medium. According to Hameed et al. [11], the Debye length ($\lambda_D$) is directly related to square root of electron's temperature and inversely proportional to electron density, as

$$\lambda_D = \sqrt{\frac{\epsilon_0 K_B T_e}{n_e e^2}} = 7430 \times \sqrt{\frac{T_e}{n_e}} \qquad (4)$$

where $\lambda_D <<< L$; $L$ represents system dimension (in cm) [12]

The Debye length must be very small. The next requirement for plasma formation is $N_D >>> 1$, where $N_D$ is the number of particles, which depends on the electron temperature and density [13]:

$$N_D = \frac{4}{3}\pi n_e \lambda_D^3 \qquad (5)$$

The objective of this study is to study the characteristics of the plasma using the spectral lines emitted from undoped cadmium oxide and copper-doped cadmium oxide targets.

## 2. Experimental Part

In this research, highly-pure (99.999%) cadmium oxide powder supplied by Sigma-Aldrich was used to make the target with a 0.3 cm thickness and 1.5 cm diameter using a hydraulic piston. Second target was made by mixing cadmium oxide with 0.5% copper. The plasma has been formed by using a pulsed Nd:YAG laser with 1064nm wavelength and 6Hz repetition rate. The laser beam was directed on the target surface at 45° angle. A plasma plume was produced above target surface when laser beam evaporated and ionized target material. Temperature, density, and plasma frequency of the electrons were measured using the OES method. Mathematical calculations were used to determine the Debye number and Debye length. Commonly used spectrometers need to be quick and have consistent response times across all shots. Therefore, a S3000-UV-IR spectrometer was used, which is characterized by its high efficiency in determining the emission wavelengths. For each spectrum, a wavelength range of 200-700nm was acquired. Undoped CdO, Cu and Cu-doped CdO targets were used to produce plasma with three different values of laser energy (500, 600 and 700mJ). As indicated in tables (1) and (2), the results were examined and compared to the National Institute of Standards (NIST) database [14-16]. The NIST database is used to identify transitions.

**Table (1) NIST standard for undoped CdO target**

| λ(nm) | Intensity | $A_{ji}.g_j$ |
|---|---|---|
| 326.10548 | 1.22E+06 | 3.80087034 |
| 340.36521 | 2.30E+08 | 7.3752952 |
| 346.61996 | 6.00E+08 | 7.3767954 |
| 361.05077 | 9.10E+08 | 7.379041 |
| 467.81493 | 3.90E+07 | 6.3831999 |
| 479.99123 | 1.20E+08 | 6.3831999 |
| 508.58217 | 1.70E+08 | 6.3831999 |
| 643.84695 | 3.00E+08 | 7.3423112 |

**Table (2) NIST standard for Cu-doped CdO target**

| λ(nm) | Intensity | $A_{ji}.g_j$ |
|---|---|---|
| 326.10548 | 1.22E+06 | 3.80087034 |
| 340.36521 | 2.30E+08 | 7.3752952 |
| 346.61996 | 6.00E+08 | 7.3767954 |
| 361.05077 | 9.10E+08 | 7.379041 |
| 467.81493 | 3.90E+07 | 6.3831999 |
| 479.99123 | 1.20E+08 | 6.3831999 |
| 508.58217 | 1.70E+08 | 6.3831999 |
| 643.84695 | 3.00E+08 | 7.3423112 |

## 3. Results and Discussion

The ionization and vaporization of target material by plasma causes a plasma plume to form across the target's surface. Due to the plasma shielding effect, which lowers the intensity of the lines, greater laser peak power levels cause the plasma to become opaque to laser beam enclosing the target. Peak intensities are different from peak to peak as a result of variations in their statistical weight, transition likelihood, and stimulated energy level. According to Boltzmann, this corresponds to the quantity of excited atoms at this level [17].

The plasma formed by the irradiation of target surface with laser beam contains excited ions and electrons. The attribution of the neutral lines that make up the plasma spectrum was performed using NIST data-base. The highest intensity spectral lines of CdO, Cu, and Cu-doped CdO in the plasma spectrum are shown in figures (1), (2) and (3). Plasma height and plasma emission rise as a result of higher ablation of the target.

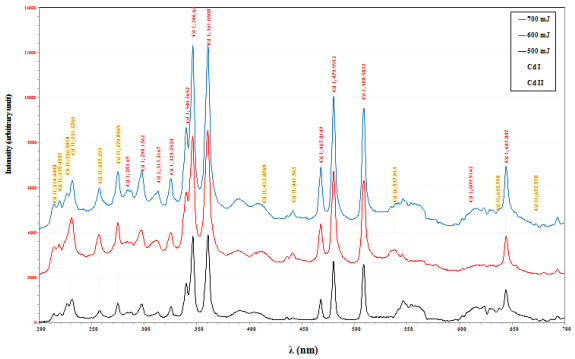


**Fig. (1) Plasma emission spectra for the undoped CdO target at different laser energies**

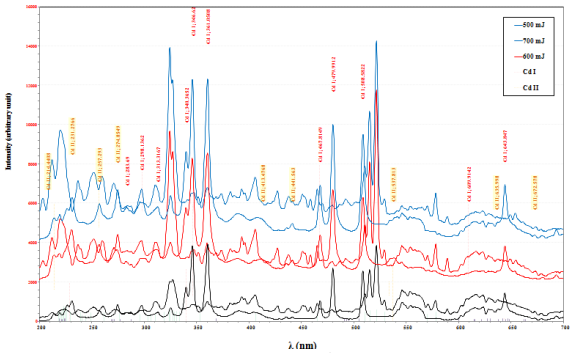


**Fig. (2) Plasma emission spectra for the pure Cu target at different laser energies**

  

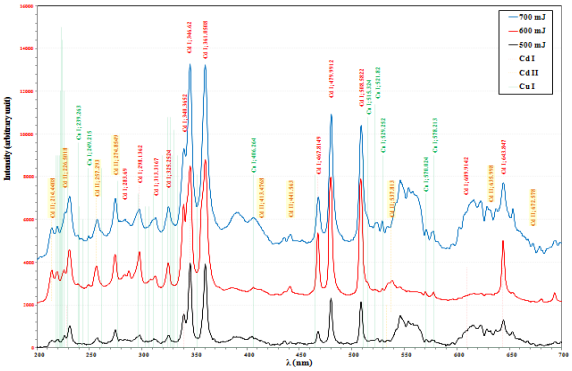


**Fig. (3) Plasma emission spectra for the Cu-doped CdO target at different laser energies**

Figures (4) (5) and (6) illustrate how the laser energy affects electron density ($n_e$) and temperature ($T_e$), which have increased with the increase of laser energy as a result of an increased probability of ionization collisions with rising electron energy ($T_e$). The target's evaporation, atomization, and focussed ionization are all caused by the laser, hence the $T_e$ is tightly connected with the laser peak power [17].

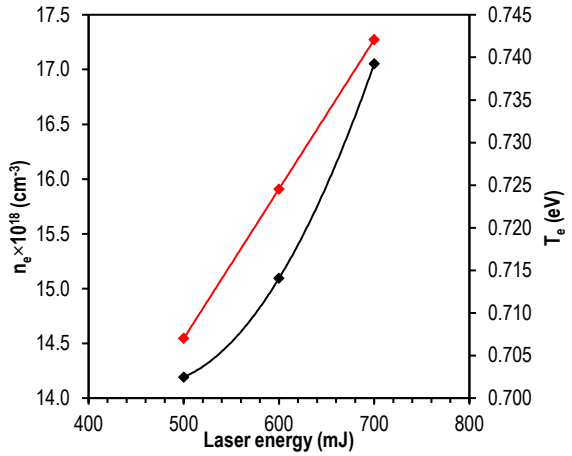


**Fig. (4) Variations of $T_e$ and $n_e$ in plasma emitted from the undoped CdO target irradiated with different laser energies**

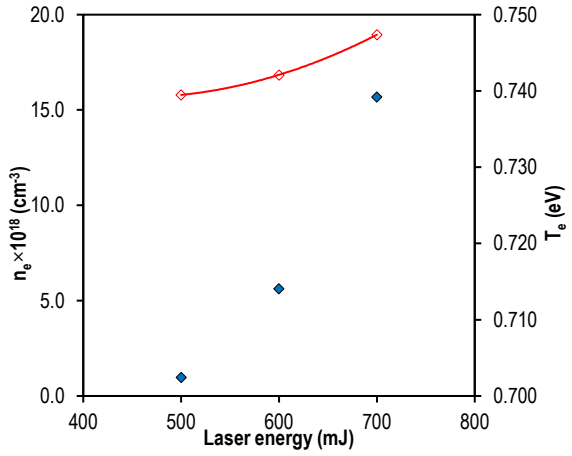


**Fig. (5) Variations of $T_e$ and $n_e$ in plasma emitted from the pure Cu target irradiated with different laser energies**

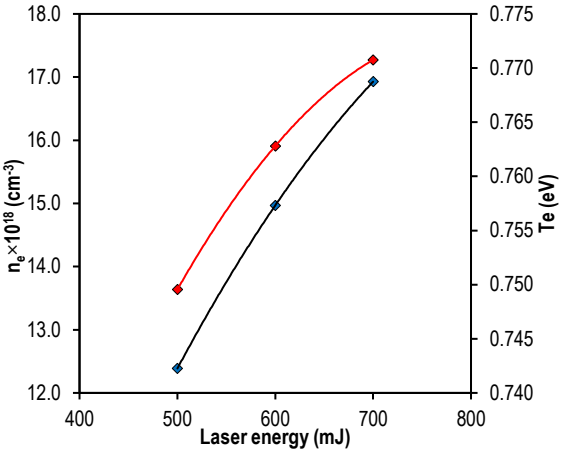


**Fig. (6) Variations of $T_e$ and $n_e$ in plasma emitted from the Cu-doped CdO target irradiated with different laser energies**

Tables (3) (4) and (5), respectively, display the computed values of $T_e$, $n_e$, $N_d$ and $\lambda_D$ for the three targets (undoped CdO, pure Cu, and Cu-doped CdO) at three different laser energies. Each estimated plasma parameter complies with the requirements and circumstances for plasma. Throughout plasma parameter outcomes ($D$, $f_p$, $n_e$), plasma has been achieved. According to Ahmed et al. [18], the plasma temperature can be calculated from Fig. (7) ($R^2$ represents statistical coefficient that indicates linearity quality). Figures (8), (9) and (10) show the relationship between intensity and wavelength showing the Lorentzian relationship at energy of 500 and 600mJ, while Gaussian at energy of 700mJ.

**Table (3) Plasma parameters for undoped CdO at various laser energies**

| E (mJ) | $T_e$ (eV) | $n_e \times 10^{18}$ (cm$^{-3}$) | $f_p$ (Hz) $\times 10^{13}$ | $\lambda_D \times 10^{-6}$ (cm) | $N_d$ |
|---|---|---|---|---|---|
| 500 | 0.702 | 14.545 | 3.425 | 1.633 | 265.24 |
| 600 | 0.714 | 15.909 | 3.582 | 1.574 | 259.91 |
| 700 | 0.739 | 17.273 | 3.732 | 1.537 | 262.75 |

**Table (4) Plasma parameters for the pure Cu at various laser energy values**

| E (mJ) | $T_e$ (eV) | $n_e \times 10^{18}$ (cm$^{-3}$) | $f_p$ (Hz) $\times 10^{13}$ | $\lambda_D \times 10^{-6}$ (cm) | $N_d$ |
|---|---|---|---|---|---|
| 500 | 0.702 | 15.789 | 3.568 | 1.567 | 254.57 |
| 600 | 0.714 | 16.842 | 3.685 | 1.530 | 252.61 |
| 700 | 0.739 | 18.947 | 3.909 | 1.468 | 250.87 |

**Table (5) Plasma parameters for the Cu-doped CdO at various laser energy values**

| E (mJ) | $T_e$ (eV) | $n_e \times 10^{18}$ (cm$^{-3}$) | $f_p$ (Hz) $\times 10^{13}$ | $\lambda_D \times 10^{-6}$ (cm) | $N_d$ |
|---|---|---|---|---|---|
| 500 | 0.742 | 13.636 | 3.316 | 1.733 | 297.53 |
| 600 | 0.757 | 15.909 | 3.582 | 1.621 | 283.89 |
| 700 | 0.769 | 17.273 | 3.732 | 1.567 | 278.64 |

  

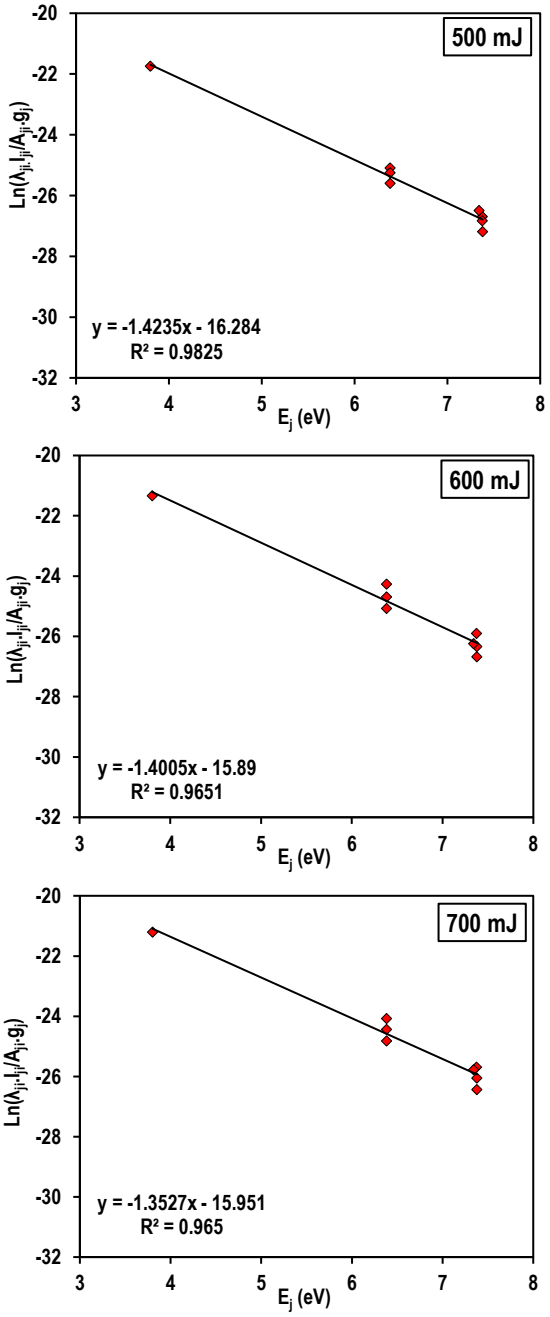


**Fig. (7) Boltzmann diagram of plasma emission from Cu-doped CdO target at energies of 500, 600 and 700mJ**

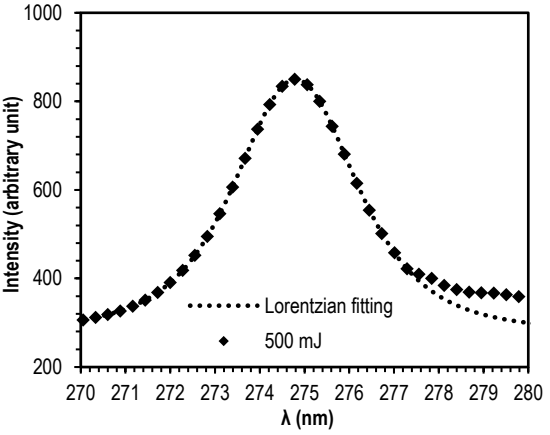


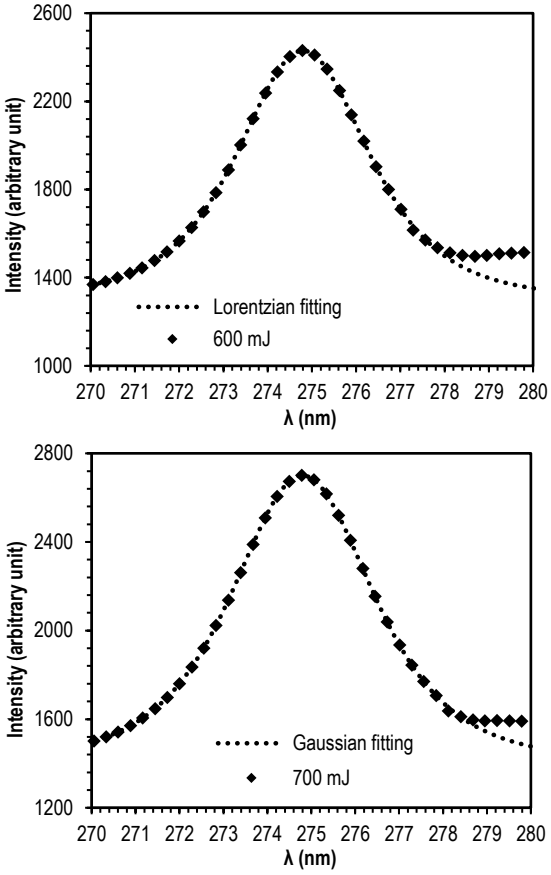


**Fig. (8) Variation of intensity with wavelength for undoped CdO target**

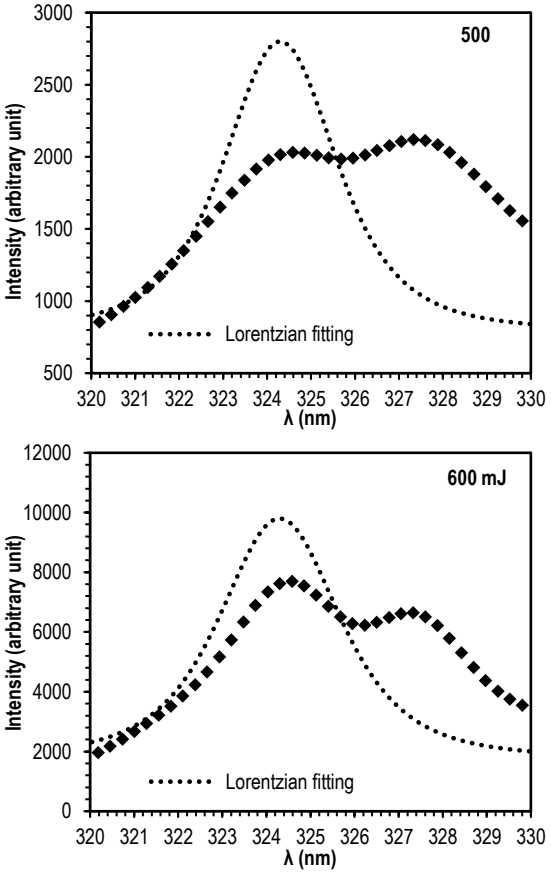


  

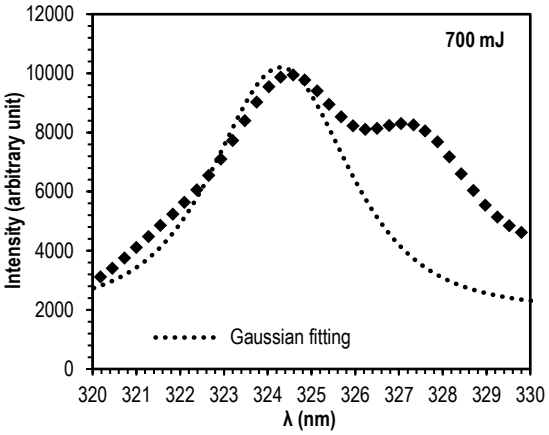


**Fig. (9) Variation of intensity to wavelength for Cu target**

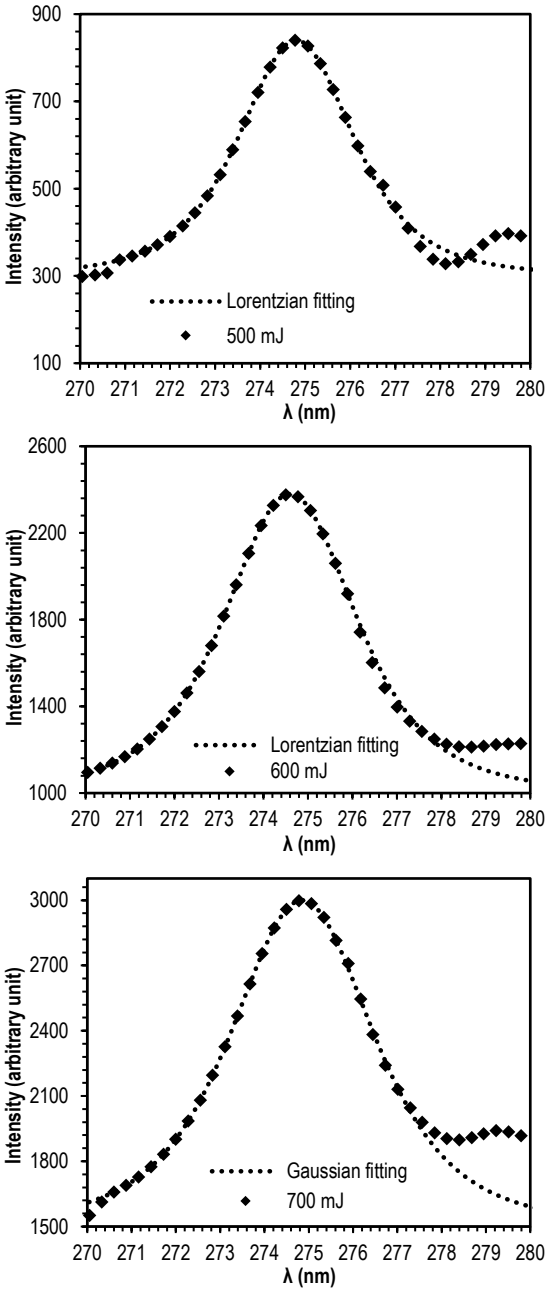


**Fig. (10) Variation of intensity to wavelength for Cu-doped CdO target**

## 4. Conclusion

Plasma was produced using a laser directed at a plate. The Intensity of the Spectral line was shown depend on laser energies, as it increased with increasing power. The plasma coefficients were estimated based on the laser energy. The results indicate an increase in the values of electron energy and electron temperature, except for the Debye length, which suffers from a decrease.

## Acknowledgment

The authors extend their thanks to the University of Baghdad, Department of Physics, and in particular the plasma laboratory for facilitating work on the devices. I also extend my thanks to Dr. Raghad and Dr. Ibrahim for the notes and advice provided by them, which facilitated the work.

## Reference

[1] G. Galbacs, V. Budavari and Z. Geretovszky, "Multi-pulse laser-induced plasma spectroscopy using a single laser source and a compact spectrometer", *J. Anal. Atom. Spectro.*, 20(9) (2005) 974-980.

[2] O.A. Hammadi, "Analysis of Secondary Electron Emission in Gas Glow Discharges Used for Thin Film Deposition Processes", *Iraqi J. Appl. Phys.*, 16(1) (2020) 15-20.

[3] A. Safeen et al., "Measurement of plasma parameters for copper using laser induced breakdown spectroscopy", *Dig. J. Nanomater. Biostruct.*, 14(1) (2019) 29-35.

[4] O.A. Hammadi, "Using Third-Harmonic Radiation of Nd:YAG Laser to Fabricate High-Quality Microchannels for Biomedical Applications", *Optik Int. J. Light Electron Opt.*, 208 (2020) 164147.

[5] B. Kearton and Y. Mattley, "Sparking new applications of laser-induced breakdown spectroscopy", *Nat. Photon.*, 2(9) (2008) 537-540.

[6] V.K. Unnikrishnan et al., "Measurements of plasma temperature and electron density in laser-induced copper plasma by time-resolved spectroscopy of neutral atom and ion emissions", *Pramana Indian J. Phys.*, 74(6) (2010) 983-993.

[7] D.A. Cremers and L.J. Radziemski, **"Handbook of laser-induced breakdown spectroscopy"**, John Wiley & Sons (2013).

[8] S.A. Mansour, "Self-absorption effects on electron temperature-measurements utilizing laser induced breakdown spectroscopy techniques", *Opt. Photon. J.*, 5(3) (2015) 79.

[9] K.A. Aadim, "Spectroscopic study the plasma parameters for $SnO_2$ doped ZnO prepared by pulse Nd:YAG laser deposition", *Iraqi J. Phys.*, 17(42) (2019) 125-135.

[10] F.F. Chen, **"Introduction to Plasma Physics and Controlled Fusion"**, Plenum Press (NY, 1984) 19-51.

  

[11] T.A. Hameed and S.J. Kadhem, "Plasma diagnostic of gliding arc discharge at atmospheric pressure", *Iraqi J. Sci.*, 60(12) (2019) 2649-2655.
[12] B.M. Smirnov, **"Physics of Ionized Gases"**, John Wiley & Sons (2008).
[13] G.H. Jihad and K.A. Aadim, "Spectroscopic study the plasma parameters for Pb doped CuO prepared by pulse Nd:YAG laser deposition", *Iraqi J. Phys.*, 16(38) (2018) 1-9.
[14] O.O. Oyebola, "Long Wave-Infrared Laser-Induced Breakdown Spectroscopy Emissions from Potassium Chloride (KCl) and Sodium Chloride (NaCl) Tablets", *J. Sci. Res. Develop.*, 17(1) (2017) 54-56.
[15] O.A. Hamadi, "Characteristics of CdO-Si Heterostructure Produced by Plasma-Induced Bonding Technique", *Proc. IMechE, Part L, J. Mater.: Design & Appl.*, 222 (2008) 65-71.
[16] O.A. Hamadi, "Effect of Annealing on the Electrical Characteristics of CdO-Si Heterostructure Produced by Plasma-Induced Bonding Technique", *Iraqi J. Appl. Phys.*, 4(3) (2008) 34-37.
[17] K.A. Aadim, A.Z. Mohammad and M.A. Abduljabbar, "Influence of laser energy on synthesizes of CdO/NPs in a liquid environment", *IOP Conf. Ser.: Mater. Sci. Eng.*, 454 (2018) 012028.
[18] B.M. Ahmed, K.A. Aadim and M.A. Khalaf, "Verify the plasma parameters generated from the Tin material using the laser-induced plasma technique", *World Scientific News*, 144 (2020) 326-337.

  